Aleksandr G. Avramenko

CHEMICAL APPLICATIONS OF HYBRIDIZED LIGHT-MATTER STATES (A REVIEW)

Wayne State University, Department of Chemistry, Detroit, MI, United States

Interactions between light and matter are a fundamental part of chemical sciences responsible for basic photophysical processes such as phosphorescence and fluorescence. However, these photophysical phenomena occur in the «weak» limit of interaction between light and matter in which the photon and molecule interact with each other without the former fundamentally changing the physical properties of the latter. By constructing a Fabry-Perot cavity, which traps light of a certain frequency, then placing a molecule in a cavity that undergoes a molecular electron transition at the frequency of the trapped light, scientists can force strong light-matter interaction. This interaction occurs if the exchange between the light of the cavity mode and the molecule's excited state is faster than the decay rate of either state, forming a hybrid light-matter state known as a polariton. The photophysical properties of these polariton states have been of interest to scientists due to the possibility that they can allow for the modification of the reactivity of molecules without the addition of functional groups or modification of the surrounding environment. Of particular interest is the ability of polaritons to influence the potential energy surface of molecules, with polaritons showing the ability to both, suppress the photochemical reaction in molecules such as spiropyran and stilbene, while also enhancing the nonradiative relaxation rate of porphyrins. Due to their photonic nature, polaritons have also shown the ability to facilitate long range energy transfer processes in organic dye molecules. This review focuses on discussing these recent advances in a chemistry context as well as the optical design of cavities required to sustain polaritons.

Keywords: cavity, polariton, Fabry-Perot, potential energy surface, distributed Bragg reflector, exciton.

Introduction

The hybridization of light and matter can be difficult to visualize for chemists. However, the basics of polariton formation can largely be thought of in terms of the familiar molecular orbital theory in which two atomic orbitals interact to form an equal number of molecular orbitals, a bonding and an antibonding orbital, at different energy levels. Likewise, a molecule can interact with a resonant cavity photon to form two polariton energy levels, as visualized in Fig. 1. Moreover, from the analogy in Fig. 1, it is evident that hybridization can happen at any energy level as long as it matches the cavity resonance. A polariton is a hybrid light-matter state that must be described by referencing both, the photon mode, and the molecular resonance mode, as seen in Eqs. (1) and (2) [1−4]:

$$|UP\rangle = \frac{1}{\sqrt{2}}\left[|e\rangle_e |0\rangle_c + |g\rangle_e |1\rangle_c\right], \qquad (1)$$

$$|LP\rangle = \frac{1}{\sqrt{2}}\left[|e\rangle_e |0\rangle_c - |g\rangle_e |1\rangle_c\right]. \qquad (2)$$

In Eqs. (1) and (2), $|g\rangle_e$ describes the excited state of the molecular exciton being coupled while $|g\rangle_e$ is the ground state. Based on these definitions, it is clear that the hybridized light-matter state consists of an excited state lacking a cavity photon
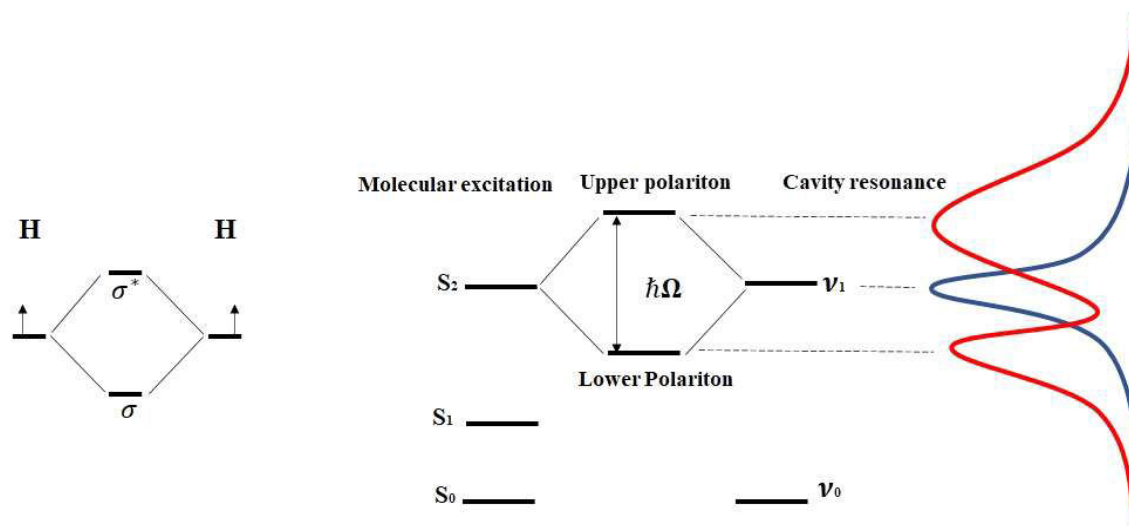
Fig. 1. The formation of a polariton can be compared to molecular orbital theory. The two atomic orbitals of a hydrogen atom can interact to form a molecule with two molecular orbitals. Similarly, a molecular excitation can interact with a cavity resonance to form an upper and a lower polariton

and a ground state with one cavity photon. In Fig. 1, the energy difference between the upper and lower polaritons is labeled as $\hbar\Omega$. This energy difference is referred to as the Rabi splitting. If dissipation is ignored, the Rabi splitting can be estimated by Eq. (3) [2,5].

$$\hbar\Omega = 2d \left(\frac{h\omega}{2 \in_0 \nu} \right)^{1/2} \left(n_{photon} + 1 \right)^{1/2}. \qquad (3)$$

In the above equation $h\omega$ is the cavity photon resonance energy, which is typically tuned to be near the near the excitation energy of the molecule to maximize the interaction between the two states, $\in_0$ is the vacuum permittivity, ν is the volume of the electromagnetic mode, and n_{photon} is the number of photons in the cavity. Based on Eq. (3), the polariton is sustained even in the absence of photons. Moreover, Eq. (3) also states that the Rabi splitting will be proportional to the square of the excitation energy. Typically, the volume of the electromagnetic mode is much larger than the volume of the molecule that is coupling to the cavity photon. Therefore, many molecules are expected to couple to a single cavity photon, increasing the Rabi splitting. Thus, the Rabi splitting will be proportional to the square root of the number of molecules (N) divided by the electromagnetic volume, or simply put, the square

of the concentration: $\hbar\Omega \propto \left(\dfrac{N}{\nu} \right) = \sqrt{C}$ [2,5]. It is

noticeable in Fig. 1 that the upper polariton has a larger full width half maximum (FWHM) than the lower polariton. Indeed, the lifetime of the polariton states is not equal, with the upper polariton typically having a shorter lifetime than the lower polariton [6,7].

Absorption occurs most efficiently when the dipole moment of a molecule and the polarization of the incident electric field are parallel [1]. Because the orientation of molecular dipoles is often randomized, there will be a large number of molecules that will form uncoupled states. These uncoupled states do not participate in polariton formation. Beside the uncoupled states, the formation of so-called «dark states» within our polariton system must also be accounted for. To visualize these «dark states» imagine that the number of molecules coupled to a cavity photon as some arbitrarily large number N. These N numbers of molecules interact with a single cavity photon, leading to the creation of a total of N+1 collective states. Out of all of the collective states, two polariton states will be formed, one UP state and one LP state, leaving a total of N−2 dark states. In simple terms, these dark states can be thought of as a superposition of molecular excitations with a very small photonic contribution. Despite not being spectroscopically observable, these states play an important role in polariton dynamics and will be discussed in further detail later in this paper.

Polariton states inherit some of the dispersive characteristics of the photon to which they are coupled to. The energy of a purely photonic state

can be described as $E_{ph}(\theta) = E_{cutoff} \left(1 - \dfrac{\sin^2\theta}{n_{eff}} \right)^{-1/2}$

[7,8]. In the aforementioned formula, E_{cutoff} is the cavity cutoff energy, or the lowest energy photon that a cavity structure can trap, defined as:

$$E_{cutoff} = \frac{hc}{2n_{eff}L}$$ [6,7,9]. In summary, the energy of

a photon changes along with a change in the wavevector of an incident wave, since it is cumbersome to experimentally measure wavevectors, relating the energy to the incidence angle of the cavity is often carried out. The energy is also related to the refractive index (n_{eff}) as well as the thickness of the cavity (L), for example, a thick cavity will be able to trap low energy photons. The dispersivity of a hybrid light-matter state formed by coupling a single exciton to a single cavity photon must be described by the two level interaction Hamiltonian shown in Eq. (4) [10]:

$$\begin{bmatrix} E_{ph} - i\sigma_{ph} & \hbar\Omega/2 \\ \hbar\Omega/2 & E_{ex} - i\sigma_{ex} \end{bmatrix} \begin{bmatrix} \alpha \\ \beta \end{bmatrix} = \in \begin{bmatrix} \alpha \\ \beta \end{bmatrix}. \quad (4)$$

In Eq. (4), the cross diagonal matrix terms $\hbar\Omega/2$ represents the coupling strength between the molecular exciton and the cavity photon. By examining Eq. (4), it is clear that there will be two for the eigenvalue, representing the UP and LP energies. Moreover, solving for the eigenvectors of this matrix would result in the calculation of the Hopfield coefficients, representing the photonic and excitonic contribution to the polariton states [11−13]. The imaginary part of the equation accounts for the FWHM of the cavity photon and exciton. Using this equation, it is possible to model the dispersion of a polariton system as seen in Fig. 2. This model assumes a $\hbar\Omega/2$ value of 150 meV and an molecular resonance excitation of 3 eV coupling to a cavity photon. It should be noted that this model assumes that a single exciton is coupling to a single cavity photon. However, cavities in which multiple excitons couple to a single cavity photon are also possible, in which case the matrix in Eq. (4) would be expanded to include the additional exciton and the interaction terms [7−14]. Moreover, the number of the final polariton states created should equal the number of starting states. Therefore, a system in which three components are involved, two excitons and one photon, would result in the formation of three polaritons, an upper, middle, and lower state. By modeling the imaginary part of Eq. (4) the FWHM of the polariton system is estimated, as seen in Fig. 3. Note that the lower polariton FWHM closely resembles the photon at low angles, and above the

resonance angle, it closely matches the exciton. The upper polariton FWHM trend is reversed, this can be easily defined by the Hopfield coefficient seen in the insert of Fig. 2. As seen from the Hopfield coefficient, the lower polariton is almost fully «light-like» at low angles, as it is tuned closer to the energy of the exciton it inherits more «exciton-like» characteristics, and at high angles the lower polariton has lost most of its «light-like» character becoming almost fully excitonic. Note that there exists a
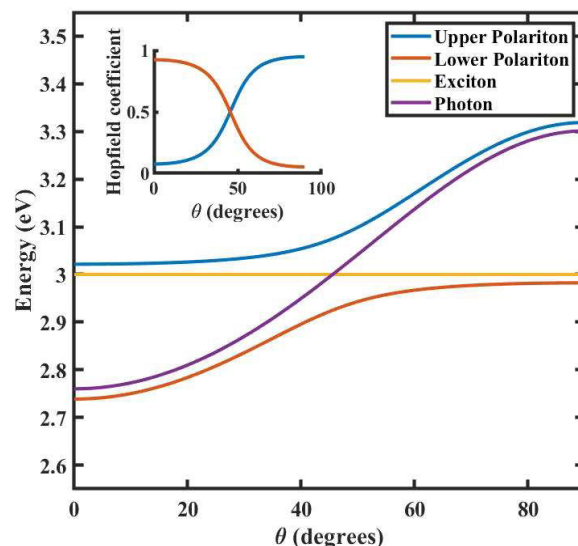

Fig. 2. Dispersion curve of a polariton formed by coupling a 3 eV excitation to a cavity photon modeled using Eq. (4). The thickness of the cavity is set such that the resonance angle is 45 degrees
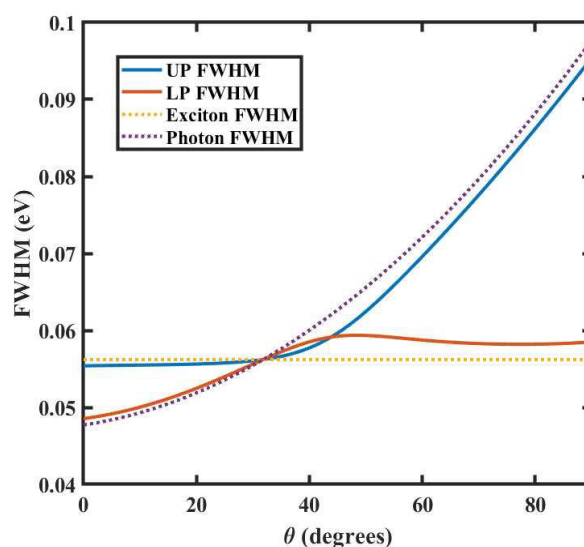

Fig. 3. The FWHM of a polariton system modeled using the imaginary part of Eq. (4)

resonance angle where both polariton states have an equal weight of photonic and excitonic character.

So far, dissipation of energy within the cavity system has not been addressed. Polaritons are sustained by energy exchange between resonant molecular and photon modes. Molecules in the excited state will naturally decay to the lowest energy state, be it by the emission of a photon or through nonradiative decay pathways. A free space molecule will have a propensity to move along the excited state potential energy surface (PES) to the lower energy ground state [15]. Just as the lifetime of the molecular excited state is finite so is the lifetime of a cavity photon. The cavity photon lifetime is limited to several femtoseconds, depending on the size and reflectivity of the cavity [16]. Because the nature of the cavity controls the characteristics of the photon mode, proper cavity design is essential in creating hybrid light-matter states.

Cavity design

Building a cavity that entraps the proper photon to exchange energy with a molecular excitation is perhaps the most important step to polariton formation. While the FWHM of the molecule is dependent on the local environment and is difficult to manipulate, it is possible to deterministically control the photon mode by manipulating the parameters of the Fabry-Perot cavity [16]. A Fabry-Perot cavity consists of two parallel mirrors separated by some distance. Light entering the structure will be repeatedly reflected by the two mirrors. Most of the light waves will be attenuated as they interfere with each other while reflecting between the two mirrors. However, there will exist a wavelength whose

l/2 is equal to the distance separating the two mirrors. The transmittance of this mode and its harmonics will be greatly amplified. The spacing between the fundamental frequency and its subsequent harmonic is referred to as the Free Spectral Range (FSR). Expressed in frequency terms it is defined as

$$FSR = \frac{c}{2nL}$$ where L is the distance between the mirrors and n is the refractive index of the spacer layer between the mirrors [16,17]. The finesse of a Fabry-Perot cavity is the relation of the Free Spectral Range to the FWHM, $F = \frac{FSR}{FWHM}$. The finesse is a measure of how narrow each resonance peak is. The higher the finesse, the narrower the resonance peaks. Moreover, the finesse connects the reflectance of the mirrors, an easily obtainable and intuitive measurement, to the FWHM and the FSR via Eq. (5):

$$F = \frac{2\pi}{\ln\left(\frac{1}{R_1 R_2}\right)}. \qquad (5)$$

A photon mode whose FWHM was matches that of the molecular mode would result in the largest number of excited state molecules interacting with the cavity photon. Because the FSR and FWHM are calculated based on the properties of the chromophore absorption peak when designing cavity polariton structures, all that is needed is to calculate the finesse and the reflectance of the mirrors using Eq. (5). The basic structure of a cavity can be seen

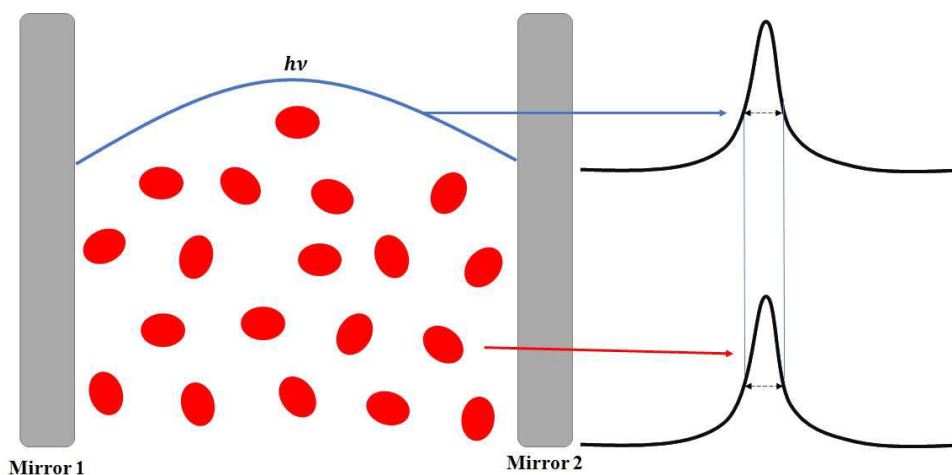

Fig. 4. The basic overview of a cavity structure in which two mirrors trap a photon (hv). The spacer layer contains a chromophore that can interact with the photon to form a polariton. The strongest coupling occurs when the FSR of the photon matches the excitation energy of the chromophore as well as when the FWHM of the photon matches the FWHM of the chromophore

in Fig. 4. One simple way to construct a cavity that could sustain a polariton would be to use two metallic mirrors and control their thicknesses.

Another important metric in cavity design is the structure's round trip attenuation coefficient. This component measures how the intensity of a photon decreases during a single round trip inside the cavity structure and is expressed by Eq. (6), in which R_1 and R_2 is the reflectively of the two mirrors forming the cavity and a is the loss coefficient $\alpha = (1/2nd)\ln\left(\dfrac{1}{R_1 R_2}\right)$. By using the information from Eqs. (5) and (6), the intensity of the photons in the cavity can be modeled using Eqs. (7) and (8).

$$r = R_1 R_2 \exp(-2\alpha nd), \qquad (6)$$

$$I_{max} = \frac{I_0}{\left((1-|r|)\right)^2}, \qquad (7)$$

$$I_{final} = \frac{I_{max}}{1+\left(\dfrac{2F}{\pi}\right)^2 \sin^2 \dfrac{\pi v_{incidence}}{v_{FSR}}}. \qquad (8)$$

Mirror design

Once the required reflectance of the mirrors has been calculated, it is necessary to properly design them. One method that has been mentioned would be to use two metallic mirrors separated by a polymer spacer layer. While this is a method that has been shown to form hybrid light-matter states, it possesses certain limitations [18]. First, metallic mirrors are thin and easily damaged. Second, common metallic mirrors such as aluminum have well known absorbance disruptions around 800 nm. Third, metallic mirrors would reflect light across a wide range of frequencies, effectively attenuating an incoming pump signal that was set to excite an off-resonance transition [19]. Perhaps most importantly, metallic films are more susceptible to damage and, as is the case for silver, which will react with oxygen to form silver oxide, resulting in the change in its reflective properties. Studies found that in a normal laboratory setting a 0.1 nm tarnished layer appeared as soon as 1 hour after deposition of a silver film, growing to 6 nm in one month [20]. By using distributed Bragg reflectors (DBRs), it is possible to more precisely manipulate the reflectance of the mirrors. DBRs are also more robust, allowing the mirror to be stored in a laboratory setting for an extended period without the mirror losing its optical

properties as well as being more resistant to mechanical damage.

To understand how reflectance and transmission is manipulated by DBRs, recall that a light wave is a periodic structure, that is, the time between two successive peaks in a light wave will be consistent. Coincidentally, when light passes through periodic medium wavelengths whose size matches the periodicity of the medium and its intensity will be attenuated [16,21]. To achieve periodicity, a DBR is typically constructed as a layered material of alternating refractive indices. A common practice is to use SiO_2 and Si_3N_4 as the periodic materials in a DBR structure due to their well-known optical properties, transparence in the visible and near IR regions, and sufficiently different refractive indices. To determine the transmission of a wave through a DBR structure, it is first necessary to understand the behavior of light at a single interface. This is achieved by utilizing the established Fresnel equations for reflectance and transmission, defined in Eqs. (9) and (10) [21]. At normal incidence, these equations simplify to Eqs. (11) and (12).

$$r_{tm} = \frac{n_1 \cos(\theta_i) - n_2 \cos(\theta_t)}{n_1 \cos(\theta_i) + n_2 \cos(\theta_t)}, \qquad (9)$$

$$t_{tm} = \frac{2n_1 \cos(\theta_i)}{n_1 \cos(\theta_i) + n_2 \cos(\theta_t)}, \qquad (10)$$

$$r = \frac{n_1 - n_2}{n_1 + n_2}, \qquad (11)$$

$$t = \frac{2n_1}{n_1 + n_2}. \qquad (12)$$

Note that dielectric materials such as SiO_2 and Si_3N_4 are chosen due to their negligible absorbance in the visible and near infrared wavelengths. These materials have a trivial contribution from the imaginary part of the refractive index in the visible region, allowing their indexes to be estimated using the Sellmeier equations, which are listed as Eq. (13) for SiO_2 and Eq. (14) for Si_3N_4. For SiO_2, the index of refraction will vary between approximately 1.47−1.45 in the 400 nm to 800 nm region, while for Si_3N_4, the index will vary between 2.1 to 2.0 over the same wavelength region [22,23]. Using the Sellmeir equations to estimate the index accounts for its variation over different wavelengths. It should be noted that metallic mirrors can also be used to

construct the cavity structure, however, metals posses an abundance of conducting electrons and Maxwell's equations must be used to simulate the optical properties of a conductive medium:

$$n^2 - 1 = \frac{0.6961663\lambda^2}{\lambda^2 - 0.0684043^2} +$$
$$+ \frac{0.4079426\lambda^2}{\lambda^2 - 0.1162414^2} + \frac{0.8974794\lambda^2}{\lambda^2 - 9.896161^2}; \quad (13)$$

$$n^2 = 1 + \frac{3.0249\lambda^2}{\lambda^2 - 0.1353406^2} + \frac{40314\lambda^2}{\lambda^2 - 1239.842^2}. \quad (14)$$

To obtain the final reflectance and transmission of a DBR structure, the Fresnel equations must be calculated at each layer of the DBR structure. To keep track of the transmission and reflectance coefficients the scatter matrix is used [16,21,24]:

$$S = \begin{bmatrix} t_{12} & r_{21} \\ r_{12} & t_{21} \end{bmatrix} = \begin{bmatrix} \dfrac{2n_1}{n_1 + n_2} & \dfrac{n_2 - n_1}{n_1 + n_2} \\ \dfrac{n_1 - n_2}{n_1 + n_2} & \dfrac{2n_2}{n_1 + n_2} \end{bmatrix}. \quad (15)$$

The t_{12} coefficient in Eq. (15) represents transmission from medium 1 to medium 2, while t_{21} represents transmission of the light back from medium 2 to medium 1. Similarly, r_{12} represents reflection from medium 1 to medium 2, while r_{21} represents reflection from medium 2 to medium 1. A single 2×2 scatter matrix represents light interaction at a single boundary of a DBR. The scatter matrix only accounts for the behavior of light through a single interface. To calculate the transmittance through the entire DBR, it is necessary to convert the scatter matrix into a wave-transfer matrix using the relationship described in Eq. (16) [16].

$$M = \begin{bmatrix} \dfrac{t_{12}t_{21} - r_{12}r_{21}}{t_{12}} & \dfrac{r_{21}}{t_{12}} \\ \dfrac{r_{12}}{t_{12}} & \dfrac{1}{t_{12}} \end{bmatrix}. \quad (16)$$

By substituting the Fresnel equations into the wave transfer matrix in Eq. (12), it is possible to solve for the transmittance of an entire DBR structure by multiplying the transfer matrices created at each boundary of the DBR. The relationship between the transmittance power and transmittance, $T_f = |t^2|$, can be used to simplify the calculation, with the final T_f of the DBR being defined by Eq. (17), in which T_i is the single segment transmission based on Fresnel equations and ψ is a factor accounting for interference inside the DBR structure defined as $\Psi = \dfrac{\sin N\varphi}{\sin\varphi}$ [16]. N is the number of DBR segments. ψ is a factor that represents single segment transmittance inside the DBR and is calculated by Eq. (18) [16].

$$T_f = \frac{T_i}{T_i + \Psi^2 [1 - T_i]}, \quad (17)$$

$$\phi = a\cos\left[\begin{array}{c} \dfrac{(n_1 + n_2)^2}{2n_1n_2}\cos(\Phi_1 + \Phi_2) - \\ -\dfrac{(n_1 - n_2)^2}{2n_1n_2}\cos(\Phi_1 - \Phi_2) \end{array} \right]. \quad (18)$$

In Eq. (18), $\Phi_1 + \Phi_2 = \dfrac{\pi\nu}{\nu_b}$ and $\Phi_1 - \Phi_2 = \dfrac{\pi\nu}{\nu_b}\left(\dfrac{n_1L_1 - n_2L_2}{n_1L_1 + n_2L_2}\right)$, where ν_b is the Bragg frequency: $\nu_b = \dfrac{c}{2(n_1L_1 + n_2L_2)}$. Finally, some conclusions of how the transmission of an incidence wave will depend on the incidence frequency, ν, can be made. First, wavelengths that are near the size of $\lambda/4n_{avg}$ will be maximally transmitted. This area of maximal transmittance is referred to as the stop band. Second, as the number of segments N increases the final transmission will decrease. This can be understood by examining the wave transfer matrix. After each successive layer, the transmission power will be reduced. Lastly, increasing the difference between n_1 and n_2 will cause an increase in the FWHM of the stop band. It should be noted that in the absence of absorption, the reflected power can be related to the transmitted power through the relationship R=1−T. However, chemists must be careful when utilizing this assumption because the creation of polaritons often requires highly absorbent materials, therefore, absorbance often must be accounted for, and the relationship Abs=1−T−R must be used [6].

History and application of strong light-matter coupling

Early studies of strong-light matter interaction involved forming hybrid light-matter states by coupling the excitons of a quantum well semiconductor to a cavity photon. The small exciton binding energy of most quantum well materials caused these structures to be highly sensitive to temperature changes [25−27]. Lidzey et al. [28] were the first to form polaritons using an organometallic molecule. The ability to strongly couple molecular excitations to resonant cavity photons presented the question of how polariton formation would impact the photochemistry and photophysics of a molecule?

Schwartz et al. [6] showed that the reaction rate of photoisomerization of a spiropyran molecule were considerably slower under strong light-matter coupling conditions. Because a molecule's reactivity is dominated by the shape of its potential energy surface (PES) it is necessary to understand how the formation of polaritons impacts its PES. If we imagine a model molecule without strong-light matter coupling, then we can assign three PESs, the ground state, V_g, the excited state V_e, and the photo-excited cavity state V_c. The V_c PES will simply be a mirror image of the ground state PES shifted by the energy of the photon: V_g+v_{ph} [29,30]. When light-matter coupling becomes sufficient, and if V_e and V_c are close in energy, then the two states can hybridize, forming a polariton PES. During hybridization, the V_c PES will inherit exciton properties from V_e, while V_e will inherit some light-like properties from V_c, as previously described by Eq. (4). This hybridization is believed to result in the polariton PES possessing a shape unique to that of either the V_e or V_c states [29,30]. In particular, because the polariton states are separated by the Rabi splitting energy, the lower polariton state is pushed down in energy in the area where the coupling is the strongest, effectively changing the energy barrier for photochemical processes. Kowalewski et al. [29] developed a formalism to describe the impact of polarton formation on the PES of excited states, allowing for scientists to carryout wave packet simulations. Galego et al. [30] and Feist et al. [31] calculated that these effects, which re-shape the polariton PES, could be used to suppress the photoisomerization reaction of a stilbene molecule.

While the aforementioned studies showed that polariton formation could be used to impact the photochemistry of molecules, they did not address what relaxation mechanisms are involved when a molecule is in the strong coupling regime and near the resonance point. Houdre et al. [32] considered how inhomogeneous (Gaussian) broadening would impact the linewidth of a polariton system. It was determined that polariton linewidths will inherit the average homogeneous lineshape $(\gamma_c+\gamma_{ex})/2$ of the photon and exciton respectively when the Rabi splitting is large. However, as the interaction between the photon and molecular modes decreases the lineshape inherits a more inhomogeneous (σ) characteristic; $(\gamma_c+\sigma_{ex})/2$. Whittaker et al. [33] observed that lineshapes of a InGaAs cavity's lower polariton are below the predicted $(\gamma_c+\sigma_{ex})/2$ value, attributing this to a motional narrowing effect. Moreover, the model described by Houdre et al. [32] predicted identical lineshapes for the upper and lower polaritons. However, it was observed on multiple occasions that the lifetime of the lower polariton was longer than that of the upper polariton [3,33−36]. Agranovich et al. [37] invoked Fermi's golden rule to explain this discrepancy in semiconductor microcavities. In summary, the rate of a quantum transition is faster to a state with higher density of final states than to a state with a lower density of final states, provided they are mediated by the same perturbation. In a polariton system, the density of dark states is large compared to that of the polariton states, allowing for a fast transition between the upper polariton and dark states. The authors also described the dark states as a broad collection of incoherent states, with the dark states assuming a «dark band» configuration. This model was further expanded by Virgili et al. [38] by additionally accounting for the changes in photon fraction with cavity detuning and the optical decay of the photons from the cavity. Based on these studies, the molecular dynamics of hybrid light-matter states are expected to be heavily impacted by the formation of the dark states. Indeed, while studying the impact of strong light-matter coupling on reverse intersystem crossing, Eizner et al. [39] reported that the rate was unchanged when the molecule was under strong light-matter coupling conditions. This was despite the energy of the lower polariton being inverted relative to that of the triplet states. The authors attributed this to the large density of states of the dark states as compared to the lower polariton. While these models provide a good approximation for the dynamics of cavity polaritons, there exists ambiguity of how these results can be applied to the photophysics and photochemistry fields. Polaritons are hybrid states, which partially inherit the nature of a molecule. However, each molecule has unique properties with a unique potential energy surface. It remains an open question how properties such as vibronic coupling between

the B and Q states in porphyrin molecules or internal conversion is impacted by polariton formation.

Wang et al. [35] showed that while fluorescence is present in the lower polariton, the nonradiative decay pathway is the dominant mechanism for the polariton state in the TDBC dye (5,6-dichloro-2-[[5,6-dichloro-1-ethyl-3-(4-sulfobutyl)benzimidazol-2-ylidene]propenyl]-1-ethyl-3-(4-sulfobutyl)-benzimidazolium hydroxide). The rate of nonradiative relaxation, such as internal conversion, is dependent on the gap law, which generally states that that the rate is proportional to the energy gap between the higher and lower lying states [40]. Despite the gap law being defined over fifty years ago, chemists still lack a deterministic way to control internal conversion through traditional synthesis methods. Avramenko and Rury [4] observed that the rates of internal conversion of a zinc (II) tetraphenyl porphyrin (ZnTPP) molecule are directly impacted by polariton formation. More specifically, the rate of internal conversion between the S_2 state of a porphyrin molecule and the S_1 states (sometimes referred to as the B and Q bands by spectroscopists) increased as the Rabi splitting was made larger. While the study demonstrated that polariton formation could exhibit rational control over internal conversion, the rates of internal conversion measured also did not match the established gap law. The reasons behind this disagreement also provide further explanation between the differences in the FWHM of the upper and lower polariton. In their work, Rury et al. report that at the appropriate Rabi splitting the ground vibrational energy level of the upper polariton overlaps with the first vibrational level of the lower polariton, allowing for maximum Frank-Condon overlap of the wavefunctions on the two energy levels, and therefore, greatly decreasing the lifetime of the upper polariton. Rury et al. also showed evidence that under strong light-matter coupling conditions the vibronic coupling between B and Q states of copper tetraphenylporphyrin (CuTPP) leads to the formation of a «Herzberg-Teller» polariton below the S_1 energy of the CuTPP molecule. The observation of a polariton energy level hundreds of millielectron volts away from that of the cavity resonance shows their potential to manipulate the energy levels of a molecule [41].

Polaritons are a hybridization of light and matter and inherit properties of both states. However, as long as the excitons meet a certain criteria such as having a matching energy with the photon and having sufficient oscillator strength, there is no set limit to how many exciton states can couple to a cavity photon. Naturally, it is easy to assume that such a structure would have some hybrid characteristic of the three or more starting states. Research on studying such multi-layer cavities has been ongoing. Lidzey et al. [14] created a multi-layer cavity system consisting of two J-aggregates whose absorption peaks were separated by 0.064 eV and were spaced apart by a 100 nm polystyrene layer. The authors observed that the photoluminescence from the lower polariton and middle polariton states varies with angle. Schwartz et al. [6] observed a similar phenomenon in that fluorescence from the lower polariton was dominant when forming polaritons using J-aggregates. However, they did not use a multi-layer cavity, coupling only one type of molecule to a cavity photon. Schwartz et al. [6] attributed their results to Kasha's rule, in which emission from the lowest lying state is expected to dominate [3]. Agranovich et al. [37] described the emission from a two level J-aggregate system that assumes the upper polariton can quickly decay into the lower branch when $\Delta E = E_{up} - E_{lp} = h\nu$ [42]. If the Rabi splitting is close to $h\nu$, then energy transfer from the upper to the lower branch can rapidly occur. Lidzey et al. [14] modified this model to describe the emission of their three level system, where energy transfer was allowed not just between the upper and lower polariton, but between the upper and middle, and middle and lower polaritons. The model produced good fits at angles below cavity resonance, however, the fit above resonance was less satisfying. Lidzey et al. [14] also demonstrated the hybridization between organic and inorganic excitons by forming cavity polaritons using J-aggregates and InGaP quantum wells. Hybridization using multiple excitons opened the possibility to creating structures, which possess chemical properties of both species. Slootsky et al. [7] expanded on this work by hybridizing two nearly degenerate exciton states of an napthalene tetracarboxylic dianhydride (NTCDA) molecule and zinc oxide (ZnO) nanoparticles. The authors concluded that the excitonic portion of the upper polariton was a mixture of the NTCDA/ZnO excitons. While the lower polariton's dominant, exciton component was the NTCDA exciton. Moreover, the authors observed an increase in the Rabi splitting of 1.44 times in the hybrid cavity over the pure NTCDA cavity, which they attributed to as evidence that both excitons couple to the cavity simultaneously [7]. Moreover, Wang et al. [43] reported coupling the Bragg modes of a DBR to the exciton of a $(PEA)_2PbI_4$ perovskite. These «Bragg polaritons» are possible in high finesse cavities and allow for the simultaneous formation of multiple polariton energy levels with unique optical properties

as each Bragg mode possesses as each Brag mode can be tuned to have a different Hopfield coefficient [43].

The impact of polariton formation on energy transfer processes such as the Forster mechanism are another area which has attracted scientific interest. The Forster resonance energy transfer (FRET) is nonradiative and relies on dipole-dipole interactions between the donor and acceptor molecules [1]. The rate of FRET is also highly sensitive to distance between the donor and acceptor molecules as well as the spectral overlap between the donor emission and acceptor absorption spectra. Recently, scientists have attempted to overcome this limitation by using hybrid light-matter states [18,44]. Zhong et al. [18] studied the energy transfer of between two dye molecules, using TDBC as a donor and a triethylammonium salt (BRK 5714) acceptor. The donor molecule had a strong absorption peak in the 590 nm region, while the acceptor molecule had a strong emission peak in the 659 nm region. The authors varied the spacer layer thickness between 10−75 nm. The authors reported that when excited outside the cavity only emission from the TDBC donor is observed. However, under strong light-matter coupling emission from both, TDBC, and BRK are observed, suggesting an energy transfer process between the two molecules is occurring [18]. Moreover, the authors reported this process occurred independent of distance. Most recently, DelPo et al. [44] concluded that the delocalized nature of polaritons can serve as an advantage in improving change transfer along a donor-acceptor interface. The authors created a bi-layer cavity using a P3HT donor and a PCBM acceptor. When excited near the dark state resonance they find the presence of a new decay pathway in their excited state absorption spectra. The new decay pathway is not present in a P3HT neat cavity, suggesting the presence of acceptor molecules is required for the observation of this pathway, and therefore, that this decay channel plays a role in charge transfer. The authors conclude that the delocalized nature of the polariton states allows for efficient donor-acceptor interaction. However, as a trade-off the charge transfer reaction is slowed. This is because while the polariton is delocalized the acceptor molecule is not. Each acceptor molecule, therefore, interacts with only a small portion of the polariton. Thus, creating a structure in which both, the donor, and acceptor, are simultaneously coupled to a cavity photon should result in efficient donor-acceptor interaction and an efficient reaction.

So far, only singlet states have been discussed while discussing the photophysics of polaritons. However, it is important to remember that triplet states also play an important role in molecular photophysics. In light emitting diodes, attempts are often made to mitigate emission due to triplet states. Researchers have attempted to use strong light-matter coupling to alter the emission of organic light emitting diodes. The Rivas group observed enhanced delayed fluorescence in tetracence crystals under strong light-matter coupling conditions [45]. However, studies by Eizner et al. [39] and Stranius et al. [11] both showed conflicting results. After creating a hybrid light-matter state by using an Erythrosine B molecule, Stranius et al. [11] reported an increase in the rate of reverse intersystem crossing (RISC) from the triplet state. On the other hand, Eizner et al. [39] measured the thermally activated delayed fluorescence and the RISC of a 3DPA3CN molecule strongly coupled to a cavity photon and reported no change in either parameter, suggesting that the photophysics of the molecule are dominated by the dark states [38]. Indeed, the polariton dark states have also been suggested to play a role in reorganizing the entropy of a polariton. For example, Scholes et al. [46] suggested that the high coherence of a polariton energy level imparted unto it by the photonic component results in a reorganization of the free energy of the system in which the polariton energy levels are higher than the dark states [38,39]. This would suggest that not only does polariton formation manipulate the spectroscopic properties of a material, but its thermodynamic properties as well. The disagreement in results also suggests that polaritons formed from coupling different molecules should not be expected to act in exactly the same manner. The light-like nature of polaritons has also been proposed by Avramenko and Spiehs [47] as a means to use visible light to destroy aquatic antibiotic contaminants, which typically require UV irradiation. This is because the UP can be tuned well above the resonance of its constituent molecule into the UV region, allowing its spectra to overlap with the contaminating molecule, initiating its photodegradation [47]. Finally, polaritons have shown promise in their ability to function as transistors [48,49]. The transistor functionally of polaritons stems from the fact that the two polariton states, UP and LP, can be well resolved, can be well separated from each other, and are optically coupled via the cavity photon, allowing the properties of one polariton to be modified by the other.

Conclusions

The goal of this paper was to introduce the reader to the basics of light-matter coupling by (1)

providing a suitable background on how a cavity photon is formed, (2) providing background on the basics of polariton photophysics, and (3) providing background on the history and current status of the field as to strong light-matter coupling is related to chemistry. The ability to manipulate the chemical landscape of a molecule with light alone provides for great possibilities in advances in such fields as optics, in which the refractive indices of a material can be manipulated by light-matter coupling. Likewise, the ability to manipulate potential energy surfaces deterministically has been a long thought-after goal in the photochemistry community as unlocking such ability would allow for the creation of novel energy storage materials. However, obstacles such as the presence of dark states and the number of uncoupled molecules remain. Moreover, it remains unclear how the nuclear, electronic, and vibrational degrees of freedom of a molecule are impacted by polariton formation. Finally, currently studies of polaritons focus on understanding their light-like properties inherited from the cavity photon. However, chemists must remember that polariton states are a hybridization of both, light and matter, and with the constituent molecular component having a major impact on the formation of the polariton state.

REFERENCES

1. *Kelley A.M.* Condensed-phase molecular spectroscopy and photophysics. − John Wiley & Sons, 2012.

2. *Ebbesen T.W.* Hybrid light-matter states in a molecular and material science perspective // Acc. Chem. Res. − 2016. − Vol.49. − No. 11. − P.2403-2412.

3. *Avramenko A.G., Rury A.S.* Quantum control of ultrafast internal conversion using nanoconfined virtual photons // J. Phys. Chem. Lett. − 2020 − Vol.11. − No. 3. − P.1013-1021.

4. Avramenko A.G., Rury A.S. Interrogating the structure of molecular cavity polaritons with resonance Raman scattering: an experimentally motivated theoretical description // J. Phys. Chem. C. − 2019. − Vol.123. − No. 50. − P.30551-30561.

5. *Modifying* chemical landscapes by coupling to vacuum fields / Hutchison J.A., Schwartz T., Genet C., Devaux E., Ebbesen T.W. // Angew. Chem. Int. Ed. − 2012. − Vol.51. − No. 7. − P.1592-1596.

6. *Polariton* dynamics under strong light-molecule coupling / Schwartz T., Hutchison J.A., Leonard J., Genet C., Haacke S., Ebbesen T.W. // ChemPhysChem. − 2013. − Vol.14. − No. 1. − P.125-131.

7. *Room* temperature Frenkel-Wannier-Mott hybridization of degenerate excitons in a strongly coupled microcavity / Slootsky M., Liu X., Menon V.M., Forrest S.R. // Phys. Rev. Lett. − 2014. − Vol.112. − No. 7. − Art. No. 076401.

8. *Holmes R.J., Forrest S.R.* Strong exciton-photon coupling and exciton hybridization in a thermally evaporated polycrystalline film of an organic small molecule // Phys. Rev. Lett. − 2004. − Vol.93. − No. 18. − Art. No. 186404.

9. *Strong* coupling between chlorosomes of photosynthetic bacteria and a confined optical cavity mode / Coles D.M., Yang Y., Wang Y., Grant R.T., Taylor R.A., Saikin S.K., Aspuru-Guzik A., Lidzey D.G., Tang J.K., and Smith J.M. // Nat. Commun. − 2014. − Vol.5. − Art. No. 5561.

10. *Skolnick M.S., Fisher T.A., Whittaker D.M.* Strong coupling phenomena in quantum microcavity structures // Semiconduct. Sci. Technol. − 1998. − Vol.13. − No. 7. − P.645.

11. *Stranius K., Hertzog M., Borjesson K.* Selective manipulation of electronically excited states through strong light−matter interactions // Nat. Commun. − 2018. − Vol.9. − No. 1. − Art. No. 2273.

12. *Graf A.*, Strong light-matter interactions and exciton-polaritons in carbon nanotubes. PhD thesis. − Heidelberg: Heidelberg University, 2019.

13. *Hopfield J.* Theory of the contribution of excitons to the complex dielectric constant of crystals // Phys. Rev. − 1958. − Vol.112. − No. 5. − Art. No. 1555.

14. *Hybrid* polaritons in strongly coupled microcavities: experiments and models / Lidzey D.G., Wenus J., Whittaker D.M., Itskos G., Stavrinou P.N., Bradley D., Murray R. // J. Lumin. − 2004. − Vol.110. − No. 4. − P.347-353.

15. *Robb M.A., Olivucci M.* Photochemical processes: potential energy surface topology and rationalization using VB arguments // J. Photochem. Photobiol. A Chem. − 2001. − Vol.144. − No. 2-3. − P.237-243.

16. *Saleh B.E., Teich M.C.* Fundamentals of photonics. − New York: John Wiley & Sons, Ltd, 2019.

17. *Kogelnik H., Li T.* Laser beams and resonators // Appl. Opt. − 1966. − Vol.5. − No. 10. − P.1550-1567.

18. *Energy* transfer between spatially separated entangled molecules / Zhong X., Chervy T., Zhang L., Thomas A., George J., Genet C., Hutchison J.A., Ebbesen T.W.// Angew. Chem. Int. Ed. − 2017. − Vol.56. − P.9034-9038.

19. *Rakic A.D.* Algorithm for the determination of intrinsic optical constants of metal films: application to aluminum // Appl. Opt. − 1995. − Vol.34. − No. 22. − P.4755-4767.

20. *Formation* and growth of tarnish on evaporated silver films / Bennett H.E., Peck R.L., Burge D.R., Bennett J.M. //

J. Appl. Phys. − 1969. − Vol.40. − No. 8. − P.3351-3360.

21. *Peatross J., Ware M.* Physics of light and optics: a free online textbook // Frontiers in Optics 2010/Laser Science XXVI. − Optica Publishing Group; 2010. − Art. No. JWA64.

22. *Malitson I.H.* Interspecimen comparison of the refractive index of fused silica // J. Opt. Soc. Am. − 1965. − Vol.55. − No. 10. − P.1205-1209.

23. *Broadband* mid-infrared frequency comb generation in a Si(3)N(4) microresonator / Luke K., Okawachi Y., Lamont M.R.E., Gaeta A.L., Lipson M. // Opt. Lett. − 2015. − Vol.40. − No. 21. − P.4823-4826.

24. *Beggs D.M.* Computational studies of one and two-dimensional photonic microstructures. PhD thesis. − Durham: Durham University, 2006.

25. *Observation* of the coupled exciton-photon mode splitting in a semiconductor quantum microcavity / Weisbuch C., Nishioka M., Ishikawa A., Arakawa Y. // Phys. Rev. Lett. − 1992. − Vol.69. − No. 23. − P.3314-3317.

26. *Spectroscopy* of polaritons in CdTe-based microcavities / Andre R., Heger D., Dang L.S., D'Aubigne Y.M. // J. Cryst. Growth. − 1998. − Vol.184-185. − P.758-762.

27. *GaAs-based* quantum well exciton-polaritons beyond 1 мм / Pieczarka M., Podemski P., Musial A., Ryczko K., Sek G., Misiewicz J., Langer F., Hofling S., Kamp M., Forchel A. // Acta Phys. Polon. A. − 2013. − Vol.124. − No. 5. − P.817-820.

28. *Strong* exciton−photon coupling in an organic semiconductor microcavity / Lidzey D.G., Bradley D., Skolnick M., Virgili T., Walker S., Whittaker D. // Nature. − 1998. − Vol.395. − No. 6697. − P.53-55.

29. *Non-adiabatic* dynamics of molecules in optical cavities / Kowalewski M., Bennett K., Mukamel S. // J. Chem. Phys. − 2016. − Vol.144. − No. 5. − Art. No. 054309.

30. *Galego J., Garcia-Vidal F.J., Feist J.* Suppressing photochemical reactions with quantized light fields // Nat. Commun. − 2016. − Vol.7. − No. 1. − Art. No. 13841.

31. *Feist J., Galego J., Garcia-Vidal F.J.* Polaritonic chemistry with organic molecules // ACS Photon. − 2018. − Vol.5. − N.o. 1. − P.205-216.

32. *Houdre R., Stanley R.P., Ilegems M.* Vacuum-field Rabi splitting in the presence of inhomogeneous broadening: resolution of a homogeneous linewidth in an inhomogeneously broadened system // Phys. Rev. A. − 1996. − Vol.53. − P.2711-2715.

33. *Motional* narrowing in semiconductor microcavities / Whittaker D.M., Kinsler P., Fisher T.A., Skolnick M.S., Armitage A., Afshar A., Sturge M., Roberts J. // Phys. Rev. Lett. − 1996. − Vol.77. − No. 23. − P.4792-4795.

34. *Exciton-polariton* dynamics in a transparent organic semiconductor microcavity / Song J.H., He Y., Nurmikko A.V., Tischler J., Bulovic V. // Phys. Rev. B. − 2004. − Vol.69. − Art. No. 235330.

35. *Quantum* yield of polariton emission from hybrid light-matter states / Wang S., Chervy T., George J., Hutchison J.A., Genet C., Ebbesen T.W. // J. Phys. Chem. Lett. − 2014. − Vol.5. − No. 8. − P.1433-1439.

36. *Motional* narrowing in semiconductor microcavities / Whittaker D., Kinsler P., Fisher T.A., Skolnick M.S., Armitage A., Afshar A., Roberts J., Hill G., Pate M. // Superlattices Microstruct. − 1997. − Vol.22. − No. 1. − P.91-96.

37. *Agranovich V.M., Litinskaia M., Lidzey D.G.* Cavity polaritons in microcavities containing disordered organic semiconductors // Phys. Rev. B. − 2003. − Vol.67. − Art. No. 085311.

38. *Ultrafast* polariton relaxation dynamics in an organic semiconductor microcavity / Virgili T., Coles D., Adawi A.M., Clark C., Michetti P., Rajendran S.K., Brida D., Polli D., Cerullo G., Lidzey D.G. // Phys. Rev. B. − 2011. − Vol.83. − Art. No. 245309.

39. *Inverting* singlet and triplet excited states using strong light-matter coupling / Eizner E., Martinez-Martinez L.A., Yuen-Zhou J., Kena-Cohen S. // Sci. Adv. 2019. − Vol.5. − No. 12. − Art. No. eaax4482.

40. *Englman R., Jortner J.* The energy gap law for radiationless transitions in large molecules // Mol. Phys. − 1970. − Vol.18. − No. 2. − P.145-164.

41. *Avramenko A.G., Rury A.S.* Light emission from vibronic polaritons in coupled metalloporphyrin-multimode cavity systems // J. Phys. Chem. Lett. − 2022. − Vol.13. − No. 18. − P.4036-4045.

42. *Experimental* study of light emission from strongly coupled organic semiconductor microcavities following nonresonant laser excitation / Lidzey D.G., Fox A.M., Rahn M.D., Skolnick M.S., Agranovich V.M., Walker S. // Phys. Rev. B. − 2002. − Vol.65. − Art. No. 195312.

43. *Room* temperature coherently coupled exciton-polaritons in two-dimensional organic-inorganic perovskite / Wang J., Su R., Xing J., Bao D., Diederichs C., Liu S., Liew T., Chen Z, Xiong Q. // ACS Nano. − 2018. − Vol.12. − No. 8. − P.8382-8389.

44. *Polariton* decay in donor-acceptor cavity systems / DelPo C.A., Khan S.U.Z., Park K.H., Kudisch B., Rand B.P., Scholes G.D. // J. Phys. Chem. Lett. − 2021. − Vol.12. − No. 40. − P.9774-9782.

45. *Enhanced* delayed fluorescence in tetracene crystals by strong light-matter coupling / Berghuis A.M., Halpin A., Le-Van Q., Ramezani M., Wang S., Murai S., Rivas J.G. // Adv. Funct. Mater. − 2019. − Vol.29. − No. 36. − Art No. 1901317.

46. *Scholes G.D., DelPo C.A., Kudisch B.* Entropy reorders polariton states // J. Phys. Chem. Lett. − 2020. − Vol.11. − No. 15. − P.6389-6395.

47. *Avramenko A., Spiehs M.* Effects of solvent environment on the spectroscopic properties of tylosin, an experimental and theoretical approach // Water Sci. Technol. − 2023. − Art. No. wst2023155.

48. *Polariton* condensate transistor switch / Gao T., Eldridge P.S., Liew T.C.H., Tsintzos S.I., Stavrinidis G., Deligeorgis G., Hatzopoulos Z., Savvidis P.G. // Phys. Rev. B. − 2012. − Vol.85. − No. 23. − Art. No. 235102.

49. *A room-temperature* organic polariton transistor /

Zasedatelev A.V., Baranikov A.V., Urbonas D., Scafirimuto F., Scherf U., Stoferle T., Mahrt R.F., Lagoudakis P.G. // Nat. Photon. − 2019. − Vol.13. − P.378-383.

ХІМІЧНІ ЗАСТОСУВАННЯ ГІБРИДИЗОВАНИХ СТАНІВ ОСВІТЛЕНОЇ РЕЧОВИНИ (ОГЛЯД)

А.Г. Авраменко

Взаємодія між світлом і речовиною є фундаментальною частиною хімічних наук, що відповідає за основні фотофізичні процеси, такі як фосфоресценція та флуоресценція. Однак ці фотофізичні явища відбуваються на «слабкій» межі взаємодії між світлом і речовиною, в якій фотон і молекула взаємодіють один з одним, не змінюючи фундаментально фізичних властивостей останньої. Сконструювавши порожнину Фабрі-Перо, яка затримує світло певної частоти, а потім помістивши молекулу в порожнину, яка зазнає молекулярного електронного переходу на частоті захопленого світла, вчені можуть ініціювати сильну взаємодію світло−матерія. Ця взаємодія відбувається, якщо обмін між світлом режиму резонатора та збудженим станом молекули є швидшим, ніж швидкість розпаду будь-якого стану, утворюючи гібридний стан світло-матерія, відомий як поляритон. Фотофізичні властивості цих поляритонних станів зацікавили вчених через можливість того, що вони можуть дозволити модифікувати реакційну здатність молекул без додавання функціональних груп або модифікації навколишнього середовища. Особливий інтерес представляє здатність поляритонів впливати на поверхню потенційної енергії молекул, причому поляритони виявляють здатність пригнічувати фотохімічну реакцію в таких молекулах, як спіропіран і стильбен, одночасно збільшуючи швидкість безвипромінювальної релаксації порфіринів. Завдяки своїй фотонній природі поляритони також продемонстрували здатність сприяти процесам передачі енергії на великі відстані в молекулах органічних барвників. Цей огляд зосереджений на обговоренні цих останніх досягнень у контексті хімічної науки, а також оптичний дизайн порожнин, необхідних для підтримки поляритонів.

Ключові слова: порожнина; поляритон; Фабрі-Перо; поверхня потенційної енергії; розподілений рефлектор Брегга; екситон.

CHEMICAL APPLICATIONS OF HYBRIDIZED LIGHT-MATTER STATES (A REVIEW)

Aleksandr G. Avramenko

Wayne State University, Department of Chemistry, Detroit, MI, United States

e-mail: aavramen@wayne.edu

Interactions between light and matter are a fundamental part of chemical sciences responsible for basic photophysical processes such as phosphorescence and fluorescence. However, these photophysical phenomena occur in the «weak» limit of interaction between light and matter in which the photon and molecule interact with each other without the former fundamentally changing the physical properties of the latter. By constructing a Fabry-Perot cavity, which traps light of a certain frequency, then placing a molecule in a cavity that undergoes a molecular electron transition at the frequency of the trapped light, scientists can force strong light-matter interaction. This interaction occurs if the exchange between the light of the cavity mode and the molecule's excited state is faster than the decay rate of either state, forming a hybrid light-matter state known as a polariton. The photophysical properties of these polariton states have been of interest to scientists due to the possibility that they can allow for the modification of the reactivity of molecules without the addition of functional groups or modification of the surrounding environment. Of particular interest is the ability of polaritons to influence the potential energy surface of molecules, with polaritons showing the ability to both, suppress the photochemical reaction in molecules such as spiropyran and stilbene, while also enhancing the nonradiative relaxation rate of porphyrins. Due to their photonic nature, polaritons have also shown the ability to facilitate long range energy transfer processes in organic dye molecules. This review focuses on discussing these recent advances in a chemistry context as well as the optical design of cavities required to sustain polaritons.

Keywords: cavity; polariton; Fabry-Perot; potential energy surface; distributed Bragg reflector; exciton.

REFERENCES

1. Kelley AM. *Condensed-phase molecular spectroscopy and photophysics*. John Wiley & Sons; 2012.

2. Ebbesen TW. Hybrid light-matter states in a molecular and material science perspective. *Acc Chem Res*. 2016; 49(11): 2403-2412. doi: 10.1021/acs.accounts.6b00295.

3. Avramenko AG, Rury AS. Quantum control of ultrafast internal conversion using nanoconfined virtual photons. *J Phys Chem Lett*. 2020; 11(3): 1013-1021. doi: 10.1021/acs.jpclett.9b03447.

4. Avramenko AG, Rury AS. Interrogating the structure of molecular cavity polaritons with resonance Raman scattering: an experimentally motivated theoretical description. *J Phys Chem C*. 2019; 123(50): 30551-30561. doi: 10.1021/acs.jpcc.9b08716.

5. Hutchison JA, Schwartz T, Genet C, Devaux E, Ebbesen TW. Modifying chemical landscapes by coupling to vacuum fields. *Angew Chem Int Ed*. 2012; 51(7): 1592-1596. doi: 10.1002/anie.201107033.

6. Schwartz T, Hutchison JA, Leonard J, Genet C, Haacke S, Ebbesen TW. Polariton dynamics under strong light-molecule coupling. *ChemPhysChem*. 2013; 14(1): 125-131. doi: 10.1002/cphc.201200734.

7. Slootsky M, Liu X, Menon VM, Forrest SR. Room temperature Frenkel-Wannier-Mott hybridization of degenerate excitons in a strongly coupled microcavity. *Phys Rev Lett*. 2014; 112(7): 076401. doi: 10.1103/PhysRevLett.112.076401.

8. Holmes RJ, Forrest SR. Strong exciton-photon coupling and exciton hybridization in a thermally evaporated polycrystalline film of an organic small molecule. *Phys Rev Lett*. 2004; 93(18): 186404. doi: 10.1103/PhysRevLett.93.186404.

9. Coles DM, Yang Y, Wang Y, Grant RT, Taylor RA, Saikin SK, et al. Strong coupling between chlorosomes of photosynthetic bacteria and a confined optical cavity mode. *Nat Commun*. 2014; 5: 5561. doi: 10.1038/ncomms6561.

10. Skolnick MS, Fisher TA, Whittaker DM. Strong coupling phenomena in quantum microcavity structures. *Semiconduct Sci Technol*. 1998; 13(7): 645. doi: 10.1088/0268-1242/13/7/003.

11. Stranius K, Hertzog M, Borjesson K. Selective manipulation of electronically excited states through strong light−matter interactions. *Nat Commun*. 2018; 9: 2273. doi: 10.1038/s41467-018-04736-1.

12. Graf A. *Strong light-matter interactions and exciton-polaritons in carbon nanotubes* [dissertation]. [Heidelberg]: Heidelberg University; 2019.

13. Hopfield J. Theory of the contribution of excitons to the complex dielectric constant of crystals. *Phys Rev*. 1958; 112(5): 1555. doi: 10.1103/PhysRev.112.1555.

14. Lidzey DG, Wenus J, Whittaker DM, Itskos G, Stavrinou PN, Bradley D, et al. Hybrid polaritons in strongly coupled microcavities: experiments and models. *J Lumin*. 2004; 110(4): 347-353. doi: 10.1016/j.jlumin.2004.08.031.

15. Robb MA, Olivucci M. Photochemical processes: potential energy surface topology and rationalization using VB arguments. *J Photochem Photobiol A Chem*. 2001; 144(2-3): 237-243. doi: 10.1016/S1010-6030(01)00453-1.

16. Saleh BE, Teich MC. *Fundamentals of photonics*. New York: John Wiley & Sons, Ltd; 2019.

17. Kogelnik H, Li T. Laser beams and resonators. *Appl Opt*. 1966; 5(10): 1550-1567. doi: 10.1364/AO.5.001550.

18. Zhong X, Chervy T, Zhang L, Thomas A, George J, Genet C, et al. Energy transfer between spatially separated entangled molecules. *Angew Chem Int Ed*. 2017; 56: 9034-9038. doi: 10.1002/anie.201703539.

19. Rakic AD. Algorithm for the determination of intrinsic optical constants of metal films: application to aluminum. *Appl Opt*. 1995; 34(22): 4755-4767. doi: 10.1364/AO.34.004755.

20. Bennett HE, Peck RL, Burge DK, Bennett JM. Formation and growth of tarnish on evaporated silver films. *J Appl Phys*. 1969; 40(8): 3351-3360. doi: 10.1063/1.1658187.

21. Peatross J, Ware M. Physics of light and optics: a free online textbook. In: *Frontiers in Optics 2010/Laser Science XXVI*. Optica Publishing Group; 2010; JWA64.

22. Malitson IH. Interspecimen comparison of the refractive index of fused silica. *J Opt Soc Am*. 1965; 55(10): 1205-1209. doi: 10.1364/JOSA.55.001205.

23. Luke K, Okawachi Y, Lamont MRE, Gaeta AL, Lipson M. Broadband mid-infrared frequency comb generation in a Si(3)N(4) microresonator. *Opt Lett*. 2015; 40(21): 4823-4826. doi: 10.1364/OL.40.004823

24. Beggs DM. *Computational studies of one and two-dimensional photonic microstructures* [dissertation]. [Durham]: Durham University; 2006.

25. Weisbuch C, Nishioka M, Ishikawa A, Arakawa Y. Observation of the coupled exciton-photon mode splitting in a semiconductor quantum microcavity. *Phys Rev Lett*. 1992; 69(23): 3314-3317. doi: 10.1103/PhysRevLett.69.3314.

26. Andry R, Heger D, Dang LS, D'Aubigne YM. Spectroscopy of polaritons in CdTe-based microcavities. *J Cryst Growth*. 1998; 184-185: 758-762. doi: 10.1016/S0022-0248(98)80158-9.

27. Pieczarka M, Podemski P, Musial A, Ryczko K, Sek G, Misiewicz J, et al. GaAs-based quantum well exciton-polaritons beyond 1 mm. *Acta Phys Polon A*. 2013; 124(5): 817-820. doi: 10.12693/APHYSPOLA.124.817.

28. Lidzey DG, Bradley DDC, Skolnick MS, Virgili T, Walker S, Whittaker DM. Strong exciton−photon coupling in an organic semiconductor microcavity. *Nature*. 1998; 395: 53-55. doi: 10.1038/25692.

29. Kowalewski M, Bennett K, Mukamel S. Non-adiabatic dynamics of molecules in optical cavities. *J Chem Phys*. 2016; 144(5): 054309. doi: 10.1063/1.4941053.

30. Galego J, Garcia-Vidal FJ, Feist J. Suppressing photochemical reactions with quantized light fields. *Nat Commun*. 2016; 7: 13841. doi: 10.1038/ncomms13841.

31. Feist J, Galego J, Garcia-Vidal FJ. Polaritonic chemistry with organic molecules. *ACS Photon*. 2018; 5(1): 205-216. doi: 10.1021/acsphotonics.7b00680.

32. Houdre R, Stanley RP, Ilegems M. Vacuum-field Rabi splitting in the presence of inhomogeneous broadening: resolution of a homogeneous linewidth in an inhomogeneously broadened system. *Phys Rev A*. 1996; 53(4): 2711-2715. doi: 10.1103/physreva.53.2711.

33. Whittaker DM, Kinsler P, Fisher TA, Skolnick MS, Armitage A, Afshar A, et al. Motional narrowing in semiconductor microcavities. *Phys Rev Lett*. 1996; 77(23): 4792-4795. doi: 10.1103/PhysRevLett.77.4792.

34. Song JH, He Y, Nurmikko AV, Tischler J, Bulovic V. Exciton-polariton dynamics in a transparent organic semiconductor microcavity. *Phys Rev B*. 2004; 69: 235330. doi: 10.1103/PhysRevB.69.235330.

35. Wang S, Chervy T, George J, Hutchison JA, Genet C, Ebbesen TW. Quantum yield of polariton emission from hybrid light-matter states. *J Phys Chem Lett*. 2014; 5(8): 1433-1439. doi: doi: 10.1021/jz5004439.

36. Whittaker D, Kinsler P, Fisher TA, Skolnick MS, Armitage A, Afshar AM, et al. Motional narrowing in semiconductor microcavities. *Superlattices Microstruct*. 1997; 22: 91-96. doi: 10.1006/spmi.1996.0275.

37. Agranovich VM, Litinskaia M, Lidzey DG. Cavity polaritons in microcavities containing disordered organic semiconductors. *Phys Rev B*. 2003; 67: 085311. doi: 10.1103/PhysRevB.67.085311.

38. Virgili T, Coles D, Adawi AM, Clark C, Michetti P, Rajendran SK, et al. Ultrafast polariton relaxation dynamics in an organic semiconductor microcavity. *Phys Rev B*. 2011; 83: 245309. doi: 10.1103/PhysRevB.83.245309.

39. Eizner E, Martinez-Martinez LA, Yuen-Zhou J, Kena-Cohen S. Inverting singlet and triplet excited states using strong light-matter coupling. *Sci Adv*. 2019; 5(12): eaax4482. doi: 10.1126/sciadv.aax4482.

40. Englman R, Jortner J. The energy gap law for radiationless transitions in large molecules. *Mol Phys*. 1970; 18(2): 145-164. doi: 10.1080/00268977000100171.

41. Avramenko AG, Rury AS. Light emission from vibronic polaritons in coupled metalloporphyrin-multimode cavity systems. *J Phys Chem Lett.* 2022; 13(18): 4036-4045. doi: 10.1021/acs.jpclett.2c00353.

42. Lidzey DG, Fox AM, Rahn MD, Skolnick MS, Agranovich VM, Walker S. Experimental study of light emission from strongly coupled organic semiconductor microcavities following nonresonant laser excitation. *Phys Rev B.* 2002; 65: 195312. doi: 10.1103/PhysRevB.65.195312.

43. Wang J, Su R, Xing J, Bao D, Diederichs C, Liu S, et al. Room temperature coherently coupled exciton-polaritons in two-dimensional organic-inorganic perovskite. *ACS Nano.* 2018; 12(8): 8382-8389. doi: 10.1021/acsnano.8b03737.

44. DelPo CA, Khan SUZ, Park KH, Kudisch B, Rand BP, Scholes GD. Polariton decay in donor-acceptor cavity systems. *J Phys Chem Lett.* 2021; 12(40): 9774-9782. doi: 10.1021/acs.jpclett.1c02644.

45. Berghuis AM, Halpin A, Le-Van Q, Ramezani M, Wang S, Murai S, et al. Enhanced delayed fluorescence in tetracene crystals by strong light-matter coupling. *Adv Funct Mater.* 2019; 29(36): 1901317. doi: 10.1002/adfm.201901317.

46. Scholes GD, DelPo CA, Kudisch B. Entropy reorders polariton states. *J Phys Chem Lett.* 2020; 11(15): 6389-6395. doi: 10.1021/acs.jpclett.0c02910.

47. Avramenko A, Spiehs M. Effects of solvent environment on the spectroscopic properties of tylosin, an experimental and theoretical approach. *Water Sci Technol.* 2023; wst2023155. doi: 10.2166/wst.2023.155.

48. Gao T, Eldridge PS, Liew TCH, Tsintzos SI, Stavrinidis G, Deligeorgis G, et al. Polariton condensate transistor switch. *Phys Rev B.* 2012; 85(23): 235102. doi: 10.1103/PhysRevB.85.235102.

49. Zasedatelev AV, Baranikov AV, Urbonas D, Scafirimuto F, Scherf U, Stoferle T, et al. A room-temperature organic polariton transistor. *Nat Photon.* 2019; 13: 378-383. doi: 10.1038/s41566-019-0392-8.

Aleksandr G. Avramenko